HI-85-36 No. 1

Steady-State Modeling of Absorption Heat Pumps with a Comparison to Experiments

M.O. McLinden
ASHRAE Associate Member

S.A. Klein, Ph.D.
ASHRAE Member

ABSTRACT

A modular, steady-state model for the simulation of absorption heat pumps (AHP) is presented. The model is based on detailed mass and energy balances and heat and mass transfer relationships for components of the cycle and is applied to a prototype AHP and compared with experimental data. The qualitative behavior of the simulated COP and system temperatures, compositions, and heat flows generally agrees with experimental results. The usefulness of the model in design studies is demonstrated by a factorial analysis investigating the sensitivity of the AHP to changes in design parameters.

INTRODUCTION

The absorption heat pump (AHP) is a type of heat-driven heat pump, which, through reversible absorption processes, utilizes the thermodynamic availability of a high temperature heat input to extract heat from a low temperature source and upgrade its temperatures to a useful level. While the absorption cycle has most commonly been used for refrigeration or air conditioning, it can also be used for heating. In a fuel-fired heating application, an AHP can achieve a heating coefficient of performance greater than one, thus improving on the efficiency of an advanced condensing furnace. (The heating COP is defined as the ratio of the useful heat delivered to the load to the high temperature heat input to the cycle.)

Historically, absorption machines have been designed more by a combination of art and cut-and-try methods than scientific analysis. While successful AHPs have resulted from these traditional methods, their performance could almost certainly be improved by a detailed component and cycle analysis.

A number of absorption heat pump models have been presented in the literature; several of these are sufficiently detailed to warrant mention. Koenig et al. (1971) have carried out an analysis of a gas-fired ammonia-water absorption chiller by writing mass and energy balances and heat transfer relationships for each component in the cycle. The solution was carried out by iterating between components in a fixed order and required several assumptions of system states (e.g., constant subcooling leaving the condenser).

A steady-state AHP simulation model has been developed by Murphy and Allen (1982) as part of a larger program to develop an AHP using organic working fluids. The general nature of the model is similar to that of Koenig's, except that the values of three system states (e.g., weak absorbent composition) were input for each set of test conditions. The heat exchange processes were treated with constant heat transfer coefficients or by assuming constant heat exchanger effectiveness. The results predicted by this model were in good agreement with experimental data.

Anand et al. (1982) have modeled the transient behavior of a lithium bromide-water chiller including the transient hydrodynamic processes in the various components. This model was used to study the time constants associated with chiller start-up.

M.O. McLinden, Research Assistant, University of Wisconsin, Madison (currently, Chemical Engineer, Center for Building Technology, National Bureau of Standards, Gaithersburg, MD); S.A. Klein, Professor of Mechanical Engineering, University of Wisconsin, Madison.

Vliet et al. (1981, 1982) have modeled a double-effect lithium bromide-water absorption chiller. Heat transfer coefficients are calculated from correlations or scaled as a function of flow rate for most of the heat exchangers. This model was used in a parametric study of design and operating variables. In this model, a single main program specifies the components present, the order of iteration between components, many of the component balances and, in some cases, initial guesses for stream conditions.

To varying degrees, the AHP models presented in the literature fall short of the goal of a flexible, general model, which would allow the simulation of a variety of system configurations and refrigerant-absorbent pairs. To simulate a machine that has not been built and to be fully useful in design studies, a model should require only design data as input. Assumptions of conditions (such as quality or approach to equilibrium) at certain points in the cycle or the input of system states often require test data or experience with similar machines. While a given assumption may be applicable for a given machine under normal operating conditions, it may not be true for all possible conditions or sets of component parameters. Although a major use of simulation is to study machines or configurations that have not been built, a simulation model should be validated against experimental data.

The primary objective of this work was to develop the capability to model absorption heat pumps in some detail, making as few assumptions regarding system states as practical. While an effort was made to develop a general, flexible model, a secondary objective was to model a particular absorption heat pump and compare simulation and experimental results.

SYSTEM DESCRIPTION

The absorption heat pump considered in this work was a prototype developed by an American manufacturer under government sponsorship. It is a gas-fired, heating-only, air-to-water heat pump and has been described by Kuhlenschmidt and Merrick (1983). The unit is sized for a residential application and, except for the load heat exchanger and its associated circulating pump, is contained in a single cabinet that would be located outside.

The heat pump utilizes an ammonia-water absorption cycle as shown in Figure 1. In the generator, direct firing by natural gas boils the weak absorbent returning from the absorber producing refrigerant vapor and strong absorbent. (The terms strong and weak absorbent refer to the affinity to absorb refrigerant.) The absorbent streams entering and leaving the generator are heat exchanged and the refrigerant vapor purified in the analyzer and rectifier. The rectifier employs a triple heat exchanger, which preheats the incoming weak absorbent by both cooling the exiting strong absorbent and partially condensing, and thus purifying, the refrigerant vapor.

Refrigerant condenses in the annulus of the concentric tube condenser, transferring heat to the load heat exchange stream flowing countercurrently in the inner tube. The refrigerant passes through two fixed-orifice restrictors and a concentric tube refrigerant heat exchanger as it flows to the low-side pressure of the evaporator. Two restrictors are used to provide better control of the refrigerant flow rate. The evaporator is a series-flow finned coil, which extracts heat from ambient air, vaporizing the liquid refrigerant.

A flue gas heat exchanger improves the burner efficiency by transferring heat from the combustion products to the strong absorbent stream, although at the expense of increasing the temperature and thus the vapor pressure of the absorbent entering the absorber. In the falling-film type absorber, solution absorbs refrigerant vapor supplied by the evaporator as it drips over tubes, transferring heat to the load heat exchange fluid flowing inside. The resulting weak absorbent collects in a sump at the bottom of the absorber and is returned to the high-side pressure of the generator/rectifier by the positive displacement diaphragm-type solution pump, thus completing the cycle.

The heat pump was tested at the National Bureau of Standards in an environmental chamber with controlled dew-point and dry-bulb air temperatures. Water at a constant temperature and flow rate was pumped to the unit where it flowed in parallel to the condenser and absorber. The test procedures and steady-state and cyclic performance of this machine are described by McLinden et al. (1983, 1984).

MODEL DESCRIPTION

The simulation model developed in this work is steady-state, modular, and stream-based. The modular approach was selected as being most compatible with the goal of a general, flexible model. Components in the simulation are separate subroutines (written in ASCII FORTRAN) corresponding, in most cases, to physical components in the real cycle. Each component subroutine calculates the state(s) of the leaving stream(s) given the state(s) of the input stream(s) and values for the design parameters (e.g., heat exchange area). Although the need to model the prototype AHP has led to assumptions of configuration for various components, the structure of the program allows modification of components or the addition of new components to model other systems. Property relations are referenced directly in the component routines and are supplied as separate FORTRAN subroutines, making the model independent of the working fluids.

The streams flowing between components are specified by a unique stream number. Each stream is represented as a one-dimensional array containing the stream type (e.g., a refrigerant-absorbent mixture versus a heat exchange fluid), mass flow rate, pressure, composition, enthalpy, temperature, and equilibrium vapor quality. There are also "data streams," which can be used to pass information such as a heat flow or control function between components.

An examination of the usual set of mass and energy balances and heat and mass transfer relationships revealed that they were insufficient to completely specify the state of an absorption cycle (McLinden 1984). The final two relationships are contained in a inventory balance. The absorption cycle (exclusive of external heat exchange streams) is a closed system, and thus the total charges of refrigerant and absorbent must be constant and represent two design variables. A model formulation that does not account for inventory would be underspecified and thus must make assumptions of system states to replace the inventory relationships.

The overall structure of the simulation is shown in Figure 2. The input data specifies the components present in the simulation, their parameters, and the manner in which they are connected, as well as initial guesses for system pressures. The simulation iterates between components in several iterative loops. Because of the cyclic nature of the system, initial guesses for a number of streams (called tear streams (Rudd and Watson 1978)) are required and are supplied as input information to the simulation. The calculation for an iterative loop starts with a tear stream, proceeds through a number of components (with the output streams calculated by one component being the input streams to the next), and finally returns to the tear stream. The iteration is controlled by separate convergence components which monitor the state of a given tear stream between successive iterations and return the calculations to the first component in an iteration loop if the stream has not converged within a specified tolerance. When the tear stream has converged, the iteration proceeds to the next component in the order specified in the input data.

The inventory analysis is contained in the outermost iteration loop and is paired to the low- and high-side system pressures. (This pairing represents only one possible choice. The inventory relationships represent two equations which are dependent on the conditions in the various components and thus could have been used, in principle, to set any two system variables that affect the inventory.) When the entire cycle has converged for a given set of pressures, the inventory of absorbent and refrigerant computed in each component are summed and compared to the (known) total inventory. New guesses for the pressures are then generated and the cycle iteration begins again.

Each of the components in the absorption cycle is represented by an analogous subroutine in the simulation. The analysis of the components is generally based on straightforward mass and energy balances, which will not be presented here; a complete description of the simulation program is given elsewhere (McLinden 1984). In developing the component models, pressure drops (except in restrictors and pumps) and heat losses to the surroundings are neglected. The state of all streams (except for those within the absorber) is taken to be fully specified by the stream type, pressure, composition, and enthalpy (i.e., thermodynamic equilibrium of two-phase streams is assumed). The required property relations of enthalpy, specific volume, and vapor-liquid equilibrium behavior for the ammonia-water system were derived from an equation of state presented by Schultz (1971).

The generator is treated as a fully mixed vessel with known heat input. The exiting refrigerant vapor and strong absorbent streams are assumed to be saturated and in equilibrium.

The analyzer is basically a distillation column contacting refrigerant vapor and weak absorbent with the addition of a heat exchanger (containing strong absorbent) extending the entire length of the column. It is treated as a series of N equilibrium stages. The contacting streams entering each stage are assumed to mix and leave in thermodynamic equilibrium. The heat exchange with the strong absorbent is treated with an overall heat transfer coefficient-area product.

The solution of the analyzer requires two concentric iteration loops. The outer loop employs a two-variable secant method to iterate on the mass flow rate and composition of the liquid leaving the bottom stage. The state of the weak absorbent entering the stage necessary to satisfy these guessed values of flow rate and composition are calculated by the use of an inner secant method iteration loop. The output streams of the bottom stage become the inputs to the next, and the solution proceeds stage-by-stage up the column. The convergence of the outer iteration loop is checked at the top stage.

A general heat exchanger component was developed to model the rectifier, condenser, evaporator, and refrigerant and flue gas heat exchangers in the prototype heat pump. This component treats N streams (including multi-component two-phase streams) in thermal contact. A maximum of one countercurrent and one cross-flow stream is permitted. The heat flow between co- or countercurrent flow streams is treated with a UA - log mean temperature difference formulation with the overall coefficient calculated from film coefficients, which can be supplied as (constant) parameters or calculated as a function of local conditions (e.g., quality). The concept of heat exchanger effectiveness is used for cross-flow streams.

The heat exchanger is divided into nodes and employs a fourth-order Runge-Kutta technique to solve for the enthalpy of the streams down the length of the exchanger. If a counterflow stream is present, an iteration for its outlet enthalpy is required; the computed enthalpy at the end of the heat exchanger is compared to the inlet value to check convergence. If a stream has gone from single to two-phase (or vice-versa) within a node, it is likely that the heat transfer coefficient and temperature differences between streams have changed significantly. When this occurs, the node is subdivided at the point of the phase transition. A similar checking for phase transitions was also found to be necessary for each extrapolation in the Runge-Kutta method.

The falling-film absorber component applies the analysis of Nakoryakov and Grigor'eva (1976) for the absorption of vapor into a laminar film flowing over an isothermal plate to each row of absorber heat exchange tubes. Their analysis assumes that the absorbent solution enters the top of the plate at a uniform composition and temperature (equal to the plate temperature) and equilibrium exists at the vapor-liquid interface. It assumes fully developed hydrodynamic and thermal profiles and a penetration theory approximation for mass diffusion. The vapor-liquid equilibrium behavior is linearized about the inlet conditions. The analysis yields expressions for the temperature of the liquid-vapor interface and the resulting heat and mass fluxes.

In implementing this analysis, the laminar velocity profile for flow over a cylinder was integrated to obtain an average velocity and film thickness in order to approximate flow over a tube as flow over a plate. The row-by-row calculations begin at the top. The outlet conditions of the absorbent solution for one row become the inlet conditions to the next lower row; the absorbent solution is assumed to mix fully as it drips from tube to tube. The absorbent solution entering a tube row is often warmer than the plate temperature; because this violates an assumed boundary condition, the Nakoryakov and Grigora'eva analysis will underpredict the heat flux. To avoid such an underprediction, the heat flux is also calculated using a constant heat transfer coefficient for the falling film, with the larger heat flux being used in the overall energy balance. The cumulative vapor absorption rate is computed at each row, and if it exceeds the inlet vapor mass flow rate, all subsequent rows serve only to transfer heat, not mass. The countercurrent heat exchange stream is solved in reverse. The outlet enthalpy of this stream (i.e., at the top of the absorber) is initially guessed. The net heat transer in each row is subtracted to give the enthalpy (and thus temperature) of this stream for the next lower row. The calculated enthalpy at the bottom row is compared with the inlet value and if necessary the iteration returns to the top row with a revised guess for the outlet enthalpy. Also at the bottom row, any unabsorbed vapor or liquid present in the inlet refrigerant stream is combined with the outlet weak absorbent.

The model for the fixed orifice restrictors employs an empirical fit of test data to an equation applicable to homogeneous two-phase flow through a sharp-edged orifice. The mass flow rate computed by the component for a given pressure drop will not, in general, be equal to the flow rate input to the restrictor. The restrictor is used to adjust the flow rates in various

portions of the cycle and thus a temporary violation of the restrictor mass balance occurs until the cycle has converged.

Other components in the simulation model are the pump, stream mixer and splitter, and a convergence enhancer. The solution pump is modeled as having a constant volumetric flow rate (based on inlet conditions) with a given outlet pressure. A component capable of mixing several input streams or splitting a single stream into liquid and vapor fractions was developed. While not corresponding to any physical component in the cycle, a convergence component employing a bounded Wegstein iteration method (Seader et al. 1974) for the solution of tear streams is necessary for the simulation.

The inventories of refrigerant and absorbent in the heat exchanger components (evaporator, rectifier, etc.) were calculated in parallel with the heat and mass balances on a node-by-node basis. The total volumes of the generator, analyzer, and absorber were divided into separate liquid and vapor portions with the inventory in each being based on the specific volume of the corresponding stream. Any stream (such as an external heat exchange stream) could be excluded from the inventory analysis by specifying zero for the corresponding volume parameter. The inventory contained in the pump, restrictor, and stream mixer components and connecting piping was assumed to be negligible.

SIMULATION OF THE PROTOTYPE AHP

The representation of the prototype AHP with the components of the simulation model is depicted in Figure 3. The tear streams necessary for the iteration of the cycle are the solution pump outlet, the analyzer weak absorbent inlet and outlet streams, and the evaporator refrigerant outlet (streams 2, 4, 5, and 19). These tear streams represent the minimum number possible for this system and were chosen according to the procedures given by Rudd and Watson (1968).

The parameters necessary to specify the heat pump include physical dimensions (e.g., heat exchanger areas and volumes), heat and mass transfer parameters, and general specifications for the simulation (e.g., how components are connected together). The major component parameters are given in Table 1. Detailed specifications for the prototype AHP were not available and thus it was necessary to estimate many of the parameters. Where possible, these were based on direct measurements of the unit. In some cases it was necessary to adjust parameters to give reasonable agreement with a limited number of experimental tests; the parameters were then checked with an independent set of three to five tests. Heat transfer coefficients for boiling and condensing ammonia were estimated according to the recommendations of ASHRAE (1981) and Threlkeld (1962). At vapor qualities above 90% and below 10%, the coefficients were varied linearly between the two phase value and the appropriate single phase value. Coefficients for the external heat exchange streams were estimated from the Dittus-Boelter equation at typical conditions and supplied to the simulation as constant parameters.

The use of inventory relations to set the low- and high-side system pressures was tested in two ways. The system pressures experimentally measured over a range of ambient temperatures were supplied to simulations at corresponding conditions. The resulting inventories were within 0.4 kg (0.9 lb) of a constant value but were significantly different than the total charge of approximately 4 kg (9 lb) ammonia and 7 kg (15 lb) water reported by the manufacturer.

The second test of the inventory analysis was to iterate for system pressures using calculated values for the total inventories. Starting with initial guesses for pressure 5% above and below the measured values, the pressures and inventories converged to within 0.3% of their correct values with 10 iterations of the complete cycle. This convergence demonstrates, in principle, the use of inventory analysis to calculate two system variables that otherwise would have to be assumed.

Unfortunately, however, the iteration did not reliably converge for more realistic starting guesses. The limited convergence of the inventory/pressure iteration was due primarily to simplifications made in the modeling of the component inventories. In particular, the generator and analyzer (which together held the majority of the total charge) were modeled as having fixed liquid and vapor volumes. While the total volume of these components is relatively constant, the fraction that is liquid will change with external conditions and total charge. In addition, the total cycle inventories showed considerable curvature as a function of pressure, making convergence more difficult for the linear iteration technique employed. Because of these problems, the inventory iteration was not used and experimentally measured system pressures were supplied to all further simulations presented here.

The performance of the prototype AHP was simulated at ambient and load water conditions corresponding to experimental tests, allowing for a direct comparison. For these comparisons, a COP not including burner losses or electric power input will be used; it is defined as the sum of the heat flows delivered to the load divided by the heat input to the generator plus flue gas heat exchanger.

Simulated and measured COPs are shown in Figure 4 for a range of ambient temperatures with the standard load water inlet temperature and flow rate of 41°C (106 F) and 0.38 L/s (6 gpm). The qualitative behavior of the two sets of results is similar. The simulated values are consistently high (by 0.11 at 15°C (59 F) to 0.18 at -21°C (-6 F)) with an error greater than the experimental uncertainty. As will be discussed later, uncertainties in the simulation parameters can result in an error in COP of 0.13. Apart from these uncertainties, one explanation for the discrepancy is that the model does not account for heat losses to the surroundings; inclusion of such losses would lower the COP, especially at lower ambient temperatures.

The simulated COP levels out more at high ambient temperatures but not as much at low temperatures as experimentally observed. The reason for this behavior is likely to be related to conditions in the evaporator. The 2 to 3°C (4 to 6 F) discrepancy in the evaportor inlet temperatures (stream 18) indicated in Table 2 is probably the result of a significant pressure drop between the evaporator inlet and the absorber (where the pressure was measured). Since this pressure drop was not accounted for in the model, the simulated evaporator temperature will be low, resulting in a greater temperature difference relative to the ambient. Similar effects resulting from such a pressure drop were noted by Vliet et al. (1981, 1982). At the lower ambient temperatures the greater temperature difference resulted in an increased heat flow from ambient, yielding higher simulated COPs. At the higher ambient temperatures, the evaporator outlet stream (stream 19) is nearly completely vaporized (as indicated by the temperature rise between the evaporator inlet and outlet) and thus the increased temperature difference has much less effect.

Measured and simulated temperatures for several other streams are also given in Table 2. In general, there is reasonable agreement between the values. The simulated temperature of the strong absorbent leaving the rectifier (stream 8) was consistently high (with an RMS error of 25°C (45 F)) indicating that the heat exchange area and/or heat transfer coefficient in the rectifier was underestimated. The simulated solution pump outlet (stream 2) temperature was high by an average of 11°C (20 F). This difference may be due to an underestimation of the absorber area or the high simulated strong absorbent temperature and refrigerant vapor quality inlet to the absorber.

A comparison of simulation results with measured absorbent compositions (expressed as mass fraction ammonia) and heat flows is presented in Table 3 for two ambient temperatures. The simulated strong and weak absorbent compositions were both low by 0.04, but the simulated composition difference between the two streams was only 0.005 greater than the experimentally observed value of 0.19. The simulated condenser heat flow was low by 0.2 to 0.4 kW (700 to 1400 Btu/h), corresponding to the slightly low values of refrigerant mass flow rate. The heat transfer in the evaporator was low at the high ambient temperature because of the low simulated refrigerant flow rate but high at the low ambient temperature because of a low evaporator temperature (as discussed above).

The results of simulations carried out with varying inlet load water temperature at these ambient temperatures are given in Table 4. The simulated COPs are consistently above the measured values for the reasons discussed above. The variation in COP for a change in water temperature from the standard conditions (ΔCOP), however, showed good agreement with experimental results for the two higher ambient temperatures. A lower load water temperature in the absorber results in lower absorber and evaporator pressures. At the two lower ambient temperatures, this lower evaportor pressure (and thus temperature) resulted in a larger heat flow from ambient increasing the COP. At the highest ambient temperature, the refrigerant leaving the evaporator is nearly completely vaporized for all three water temperatures and thus variations in the low side pressure had much less effect.

The sensitivity of the prototype AHP to changes in simulation parameters was studied by means of a factorial design. This analysis also served to further exercise the model and to estimate the uncertainty in COP arising from uncertainties in simulation parameters.

A factorial design is useful for investigating the effects of a number of variables (or factors) with a minimum number of experiments or simulations. The most common design, and the one employed here, varies the factors between two levels in a specified fashion. The results of the analysis are "main effects" for each factor and interactions between factors. A main

effect is the response of a dependent variable (e.g., COP) to a change from the low to high level of a factor (e.g., a heat exchanger area) taken over the average of all other factors. Interactions measure the result of two or more variables simultaneously changing from their low to high level. There are two- and three-factor interactions, up to a k-factor interaction (where k is the number of variables investigated).

To fully investigate k factors at two levels would require 2^k tests. A fractional factorial design requires fewer tests but at the expense of confounding main effects and interactions. Means are available, however, to insure that main effects (which are likely to be significant) are confounded only with high-order interactions (which are likely to be neglibible). (A thorough discussion of factorial and fractional factorial designs may be found in Box et al. (1978)).

In the study of the prototype AHP, 12 design parameters along with the low- and high-side pressure and ambient temperature were investigated with 32 simulations. In the resulting fractional factorial design, the main effects were confounded only with three-factor and higher interactions, but two-factor interactions were confounded with each other. The low and high levels of the design variables are given in Table 5. (The effects of heat transfer coefficients were lumped with those of the heat exchange areas.)

The results of this analysis, in terms of effects on COP, are given in Table 5. The average value of COP and the main effect of ambient temperature are consistent with the results presented above. An increased low-side pressure decreases the temperature difference for heat transfer in the evaporator and thus reduces COP; this is reflected in the negative value for this effect. The effect of generator heat input is negative, suggesting that the condenser and/or evaporator are not capable of handling the increased refrigerant flow rate resulting from a higher generator heat input. The effect of condenser area is significant and positive; the condenser is undersized under some conditions (as indicated by a two-phase exiting refrigerant stream) and thus the performance of the heat pump is sensitive to the condenser area. An increased high-side pressure increases the heat flow in the condenser and thus also has a positive effect on COP.

The remaining factors had effects smaller than 0.01. The relative insensitivity of performance to the analyzer, rectifier, absorber, and refrigerant heat exchange areas suggests that these components are oversized so that a relatively large (20%) change in area results in only a small performance change. The effects associated with the solution pump and throttle valve parameters are also small; it is possible that the sizing of these components was optimized in the design of the prototype AHP.

The ranges for the variables investigated in the factorial design were chosen to correspond to the uncertainties in the corresponding simulation parameters. Thus the main effects can also be interpreted as errors in the simulated COP arising from uncertainties in the parameters supplied to the model. The total error in COP (excluding the effect of ambient temperature) is 0.13. Although this value is specific to the unit investigated here, its magnitude indicates that parameters must be known to a high precision to obtain accurate results for COP. In the absence of input data of high precision, the simulation model is still useful for investigating the relative performance resulting from changes in design parameters.

In addition to the main effects, the factorial analysis yielded 16 interaction effects; of these, six had absolute values greater than 0.01. However, these interaction terms are highly confounded among the 105 two-factor interactions possible among the 15 variables. Some of these interactions were resolved by an additional factorial design carried out for identical low and high levels of five variables having significant effects on COP. (All other variables, including ambient temperature, were held at their low levels.) In this design, two-factor interactions are confounded with three-factor and higher interactions but not each other.

The average and main effects for this analysis (given in Table 6) are slightly different from the values in Table 5, indicating that there is an interaction with ambient temperature or the other variables. A number of substantial interaction effects (given in Table 7) exist among the five variables. (Table 7 also indicates the three-factor interaction with which each two-factor interaction is confounded; the given value is the sum of the two-factor and associated three-factor interaction.) For example, the interaction between condenser area and high side pressure is negative, indicating that, although each individual factor improves COP, the effect of increasing both factors simultaneously has an effect less than the sum of the individual factors. These interactions illustrate the complex nature of the absorption cycle. In designing an AHP, it is not possible to optimize components individually; rather, the cycle as a whole must be considered.

CONCLUSIONS

The modular steady-state model for absorption heat pumps developed in this work was applied to simulate a prototype AHP and has been successfully demonstrated. A comparison of experimental and simulation results generally showed good agreement, although revealing several needed refinements to the model; in particular, neglecting heat losses to the surroundings and pressure drops through components led to overpredictions of COP. An analysis of the refrigerant and absorbent inventory is needed to fully specify the state of the absorption cycle. The use of the inventory analysis to iterate for system pressures was demonstrated in principle, but in practical tests this approach was not successful due to oversimplifications in the treatment of components with changing liquid volumes.

The significant interactions present between design parameters revealed by a factorial analysis of the AHP illustrate the difficulty of optimizing an AHP and the usefulness of a simulation design tool. The factorial analysis also revealed that uncertainty in design parameters can lead to considerable uncertainty in simulated results such as COP. Accurate simulation results would require "calibration" of the model with experimental data. Although in the absence of precise parameter estimates, simulation can still reveal the relative performance resulting from changes in design variables.

REFERENCES

American Society of Heating, Refrigerating and Air Conditioning Engineers, 1981. Handbook of Fundamentals.

Anand, D.K.; Allen, R.W.; and Kumar, B. 1982. "Transient Simulation of Absorption Machines," Journal of Solar Energy Engineering, 104 197.

Box, G.E.P.; Hunter, W.G.; and Hunter, J.S. 1978. Statistics for Experimenters, John Wiley and Sons.

Koenig, K.; Gable, G.K.; and Jain, P.C. 1971. "Computer Analysis of an Aqua-Ammonia Gas-Fired Air Conditioner," Natural Gas Research and Technology Conference, American Gas Association and Institute of Gas Technology, Chicago.

Kuhlenschmidt, R., and Merrick, R.H. 1983. "An Ammonia-Water Absorption Heat Pump Cycle," ASHRAE Transactions, 88 pt 1.

McLinden, M.O. 1984. "Modeling of Absorption Heat Pumps: Solar Applications Employing Chemical Storage and Steady-State Modeling With a Comparison to Experiments," Ph.D. Thesis, Chemical Engineering, University of Wisconsin-Madison.

McLinden, M.O.; Radermacher, R.; and Didion, D.A. 1983. "A Laboratory Investigation of the Steady-State and Cyclic Performance of an Air-to-Water Absorption Heat Pump," Proceedings, Congress of the International Institute of Refrigeration, Paris.

Murphy K.P., and Allen, R.A. 1982. "Development of a Residential Gas-Fired Absorption Heat Pump System: System Computer Simulation, System Seasonal Performance Simulation and System Cost," interim report for ORNL contract 86X-24610C and GRI contract 5014-341-0113.

Nakoryakov, V.E., and Grigor'eva, N.I. 1976. "Combined Heat and Mass Transfer During Absorption in Drops and Films," Journal of Engineering Physics, 32, 243.

Rudd, D.F., and Watson, C.C. 1968. Strategies of Process Engineering, John Wiley and Sons.

Schultz, S.C.G. 1971. "Equations of State for the System Ammonia-Water for Use With Computers," Proceedings, Congress of the International Institute of Refrigeration, Washington, D.C.

Seader, J.D.; Seider, W.D.; and Pauls, A.C. 1974. "FLOWTRAN Simulation--An Introduction," Monsanto Company.

Vliet, G.C.; Lawson, M.B.; and Lithgow, R.A. 1982. "Water-Lithium Bromide Double-Effect Absorption Cooling Cycle Analysis," ASHRAE Transactions, 88 pt 1, 811.

Vliet, G.C.; Lawson M.B.; and Lithgow, R.A. 1981. "Water-Lithium Bromide Double-Effect Absorption Cooling Analysis" University of Texas at Austin, final report for DoE Contract AC03-79SF10540.

Threlkeld, J.L. 1962. Thermal Environmental Engineering, Prentice Hall.

TABLE 1
Component Parameters for the Simulation of the Prototype AHP

Generator heat input (varies with ambient temp.)	10.2-10.6 kW (34.8 - 36.2 MBtu/hr)
Analyzer - number of equilibrium stages	1
overall UA for heat exchanger	0.1 kW/°C (190 Btu/F)
Rectifier - weak absorbent to vapor HX area	0.32 m^2 (3.44 ft^2)
weak to strong absorbent HX area	0.25 m^2 (2.69 ft^2)
Heat transfer coefficients: vapor	2.0 $kW/m^2 \cdot °C$ (352 $Btu/h \cdot ft^2 \cdot F$)
strong absorbent	1.8 $kW/m^2 \cdot °C$ (317 $Btu/h \cdot ft^2 \cdot F$)
weak absorbent	2.5 $kW/m^2 \cdot °C$ (440 $Btu/h \cdot ft^2 \cdot F$)
Condenser heat exchange area	0.25 m^2 (2.69 ft^2)
Refrigerant heat exchanger area	0.16 m^2 (1.72 ft^2)
Flue gas heat exchanger UA	0.06 kW/°C (110 Btu/F)
Evaporator - refrigerant side HX area	3.2 m^2 (34.4 ft^2)
air side (fin) HX area	52.8 m^2 (622 ft^2)
Absorber - heat exchange area	1.2 m^2 (12.9 ft^2)
number of heat exchange rows	30
Solution pump mass flow rate	0.0227 kg/s (3.0 lb/min)
Heat Transfer coefficients:	
load water	7.2 $kW/m^2 \cdot °C$ (1270 $Btu/h \cdot ft^2 \cdot F$)
condensing ammonia (condenser and ref HX annulus)	
subcooled liquid	0.4 $kW/m^2 \cdot °C$ (70 $Btu/h \cdot ft^2 \cdot F$)
two-phase	8.0 $kW/m^2 \cdot °C$ (1410 $Btu/h \cdot ft^2 \cdot F$)
superheated vapor	0.1 $kW/m^2 \cdot °C$ (18 $Btu/h \cdot ft^2 \cdot F$)
evaporating ammonia (evaporator and inner tube of ref HX)	
subcooled liquid	0.16 $kW/m^2 \cdot °C$ (28 $Btu/h \cdot ft^2 \cdot F$)
two-phase	3.0 $kW/m^2 \cdot °C$ (529 $Btu/h \cdot ft^2 \cdot F$)
superheated vapor	0.1 $kW/m^2 \cdot °C$ (18 $Btu/h \cdot ft^2 \cdot F$)

TABLE 2
System Pressures and Measured and Simulated COPs and
Stream Temperatures for Varying Ambient Temperatures

Ambient Temp.	Pressure (MPa)		COP		Stream Temperatures (°C) (numbers refer to Figure 3)											
					2 (pump out)		8 (rect out)		10 (abs in)		14 (cond in)		18 (evap in)		19 (evap out)	
(°C)	low	high	test	sim	test	sim	test	sim	test	sim	test	sim	test	sim	test	sim
-21.4	0.158	2.02	0.99	1.17	38	52	57	83	73	79	76	75	-23	-24	-23	-24
-15.7	0.192	2.00	1.03	1.27	40	52	56	83	72	82	73	75	-18	-20	-18	-20
-8.0	0.243	2.01	1.18	1.43	42	56	57	86	73	86	73	78	-12	-14	-12	-14
-0.9	0.299	2.06	1.32	1.50	45	55	58	83	74	84	73	75	-7	-9	-6	-1
4.7	0.336	2.08	1.37	1.52	46	54	58	80	74	83	71	73	-3	-6	5	5
8.8	0.352	2.10	1.39	1.52	46	54	58	80	74	85	71	72	-2	-5	9	9
15.5	0.360	2.13	1.41	1.52	46	53	59	80	74	85	72	72	-1	-4	16	16

TABLE 3
Comparison of Measured and Simulated Compositions, Heat Flows, and Refrigerant Mass Flow Rate for Tests at Two Ambient Temperatures

	Ambient Temperature (°C)			
	-8.7		8.6	
	test	sim	test	sim
Compositions:				
strong absorbent	0.133	0.099	0.173	0.122
weak absorbent	0.319	0.292	0.368	0.319
Heat flows (kW):				
condenser	5.8	5.6	6.1	5.7
evaporator	2.8	3.9	6.6	5.6
absorber	8.4	8.8	10.3	10.6
Refrigerant flow rate (kg/s)	0.0051	0.0049	0.0054	0.0051

TABLE 4
System Pressures, COP, Change in COP from Standard Load Water Conditions, and Simulated Heat of Evaporation for Varying Inlet Load Water Temperature at Three Ambient Temperatures.

Temperatures (°C)		Pressures (MPa)		Simulated	ΔCOP		$\dot{Q}_{evap}$
ambient	load water	low	high	COP	test	sim	(kW)
-21.4	34.9	0.148	1.77	1.28	+0.04	+0.11	3.0
	40.7	0.158	2.02	1.17	-	-	2.0
	45.6	0.164	2.26	1.11	-0.04	-0.06	1.4
-8.0	35.1	0.223	1.81	1.50	+0.03	+0.07	5.3
	40.4	0.243	2.01	1.43	-	-	4.6
	43.3	0.245	2.16	1.36	-0.06	-0.07	3.9
8.8	35.7	0.309	1.92	1.51	-0.01	-0.01	5.6
	40.5	0.352	2.10	1.52	-	-	5.5
	44.3	0.384	2.29	1.53	+0.01	+0.01	5.5

TABLE 5
Main Effects for the Factorial Analysis of the AHP

Factor	low level	high level	Effect
Average			1.426
Ambient temperature (°C)	-8	-1	+0.071
Pressures (MPa)			
low (absorber) @T_{amb} = -8	0.231	0.255	-0.072
@T_{amb} = -1	0.284	0.314	
high (rectifier) @T_{amb} = -8	1.91	2.11	+0.063
@T_{amb} = -1	1.95	2.16	
Generator heat input (kW)	9.93	10.97	-0.035
Heat exchanger areas (m^2)			
condenser	0.20	0.30	+0.056
refrigerant HX	0.13	0.19	-0.002
evaporator	2.86	4.29	+0.055
absorber	0.95	1.42	-0.008
rectifier (s.a. to w.a.)	0.20	0.30	+0.004
rectifier (vap. to w.a.)	0.26	0.38	0.000
Analyzer UA($kW/m^2 \cdot °C$)	0.08	0.12	+0.001
Analyzer stages	1	2	+0.001
Absorber heat exchange rows	25	35	+0.004
Solution pump flow (kg/s)	0.0216	0.0238	-0.004
Throttle Parameter ($MPa\ s^2/kg^2$)	22100	24500	+0.006

TABLE 6
Main Effects for the Second Factorial Analysis of the Prototype AHP

Factor	Low Level	High Level	Effect
Average			1.387
Pressures (MPa)			
low (absorber)	0.231	0.255	-0.085
high (rectifier)	1.91	2.11	+0.032
Generator heat input (kW)	9.93	10.97	-0.046
Heat exchanger areas (m^2)			
condenser	0.20	0.30	+0.033
evaporator	2.86	4.29	+0.068

TABLE 7

Two-factor Interactions and Associated Confounded Three-Factor Interactions for the Second Factorial Analysis of the Prototype AHP

Two-Factor Interaction	(confounded with)	Value
$P_{low} \times P_{high}$	$(\dot{Q}_{gen} \times A_{cond} \times A_{evap})$	-0.027
$\dot{P}_{low} \times \dot{Q}_{gen}$	$(P_{high} \times A_{cond} \times A_{evap})$	+0.004
$P_{low} \times A_{cond}$	$(P_{high} \times \dot{Q}_{gen} \times A_{cond}$	-0.025
$P_{low} \times A_{evap}$	$(P_{high} \times \dot{Q}_{gen} \times A_{cond})$	+0.020
$P_{high} \times \dot{Q}_{gen}$	$(P_{low} \times A_{cond} \times A_{evap})$	-0.011
$P_{high} \times A_{cond}$	$(P_{low} \times \dot{Q}_{gen} \times A_{evap})$	-0.017
$P_{high} \times A_{evap}$	$(P_{low} \times \dot{Q}_{gen} \times A_{cond})$	+0.021
$\dot{Q}_{gen} \times A_{cond}$	$(P_{low} \times P_{high} \times A_{evap})$	-0.015
$\dot{Q}_{gen} \times A_{evap}$	$(P_{low} \times P_{high} \times A_{cond})$	+0.003
$A_{cond} \times A_{evap}$	$(P_{low} \times P_{high} \times \dot{Q}_{gen})$	+0.021

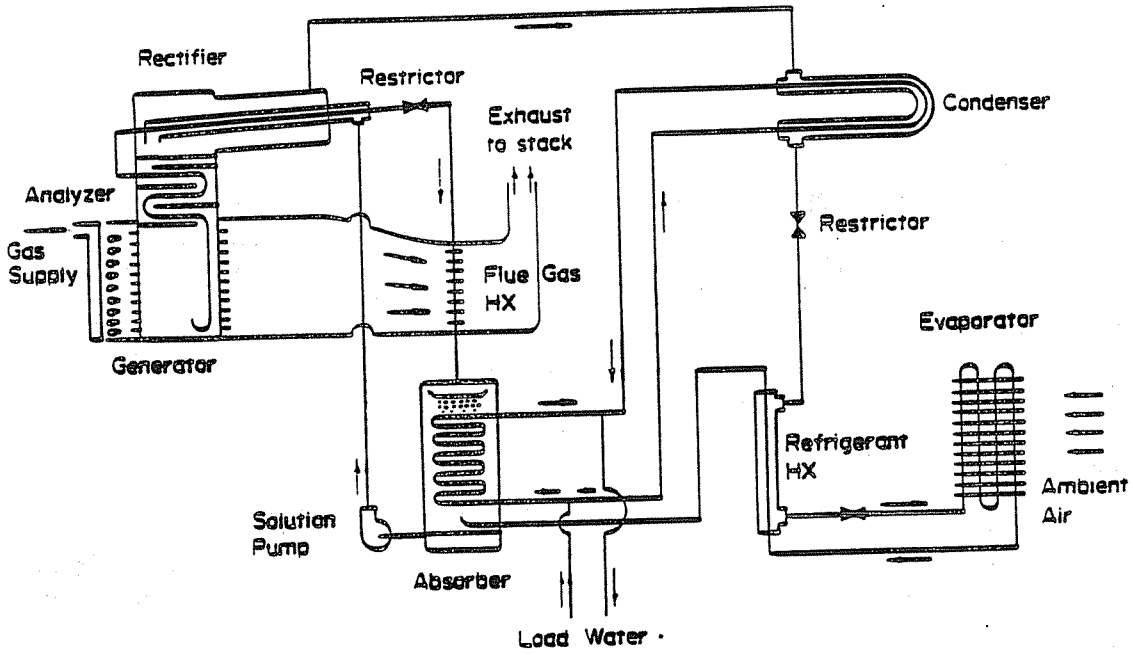

Figure 1. Schematic of the prototype absorption heat pump

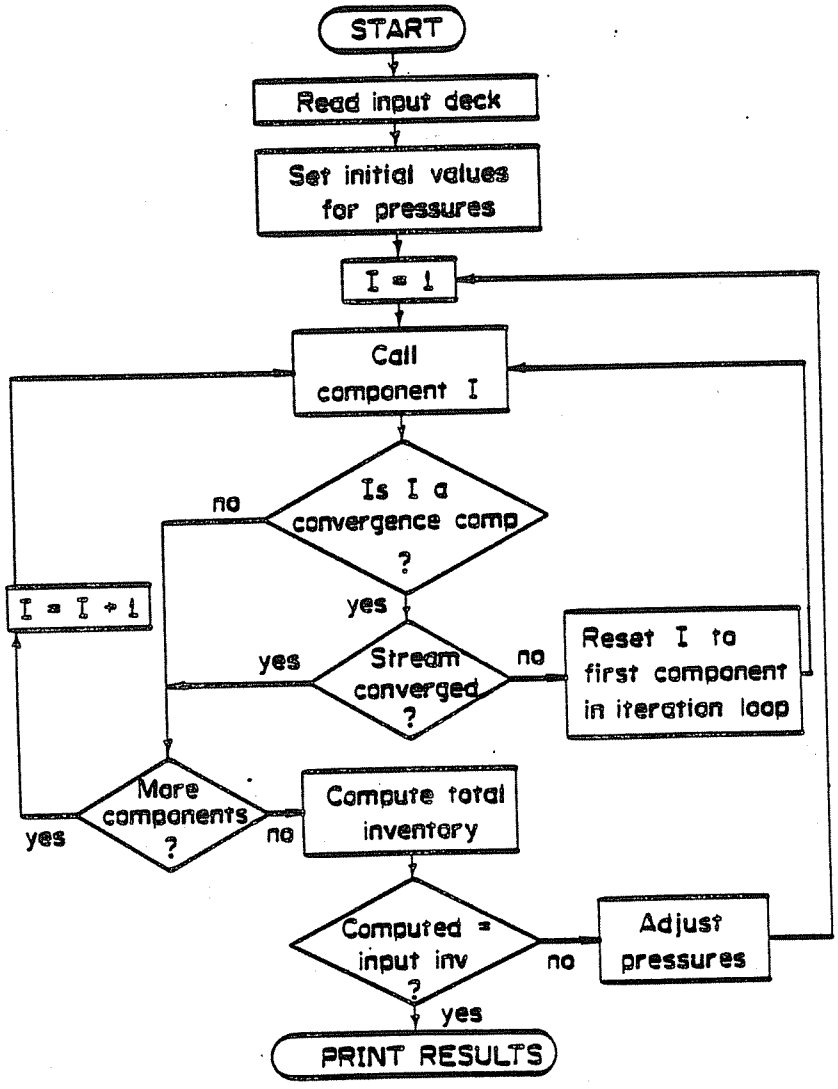

Figure 2. Overall structure of the steady-state simulation program

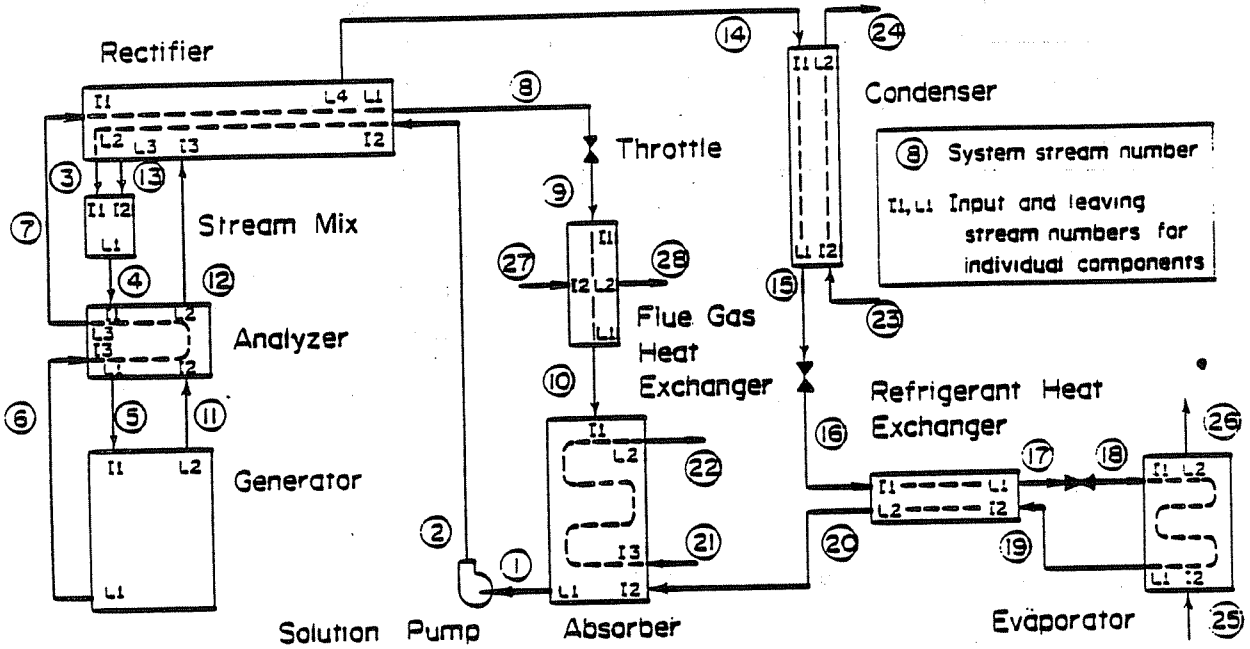

Figure 3. Simulation schematic for the prototype absorption heat pump

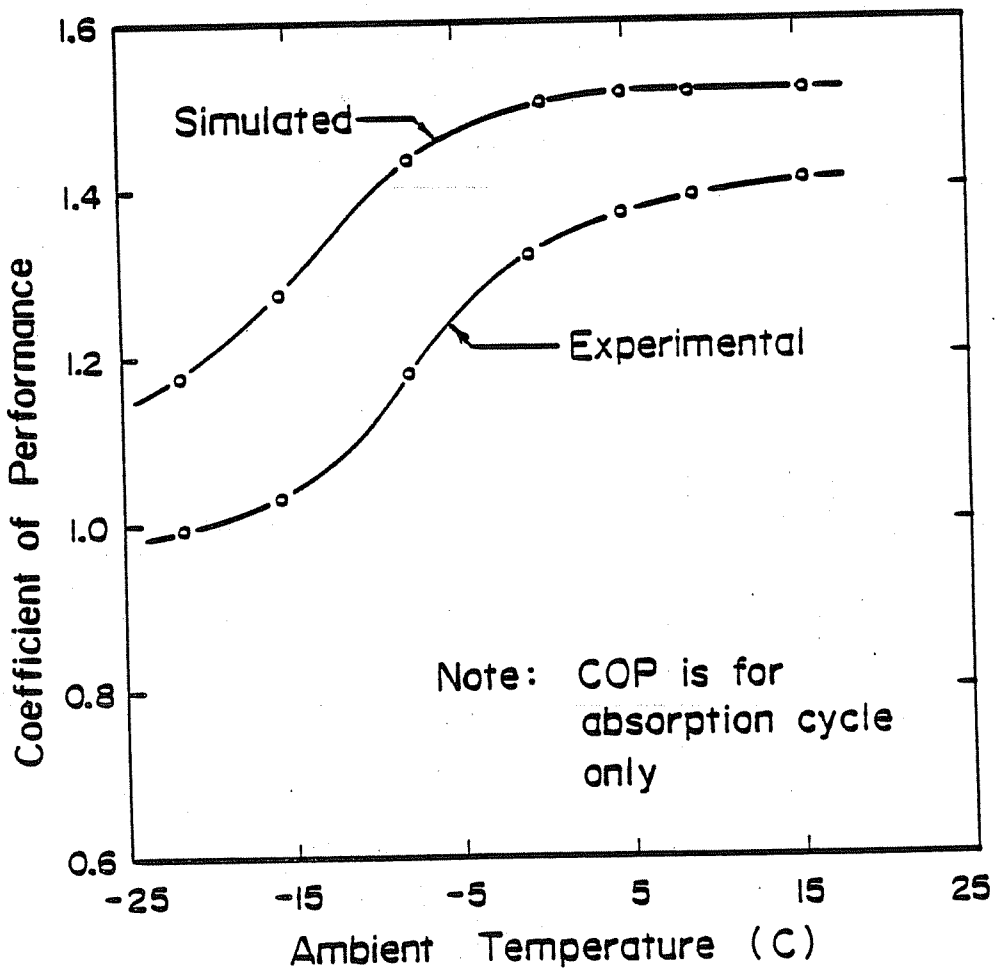

Figure 4. Measured and simulated cycle COPs for the prototype AHP as a function of ambient temperature